



**Calhoun: The NPS Institutional Archive**  
**DSpace Repository**

---

Theses and Dissertations

1. Thesis and Dissertation Collection, all items

---

1992-09

# Analytical approximation to the transmission of sound in shallow water for cross-slope propagation

Livingood, Debra M.

Monterey, California. Naval Postgraduate School

---

<https://hdl.handle.net/10945/30611>

---

This publication is a work of the U.S. Government as defined in Title 17, United States Code, Section 101. Copyright protection is not available for this work in the United States.

*Downloaded from NPS Archive: Calhoun*



<http://www.nps.edu/library>

Calhoun is the Naval Postgraduate School's public access digital repository for research materials and institutional publications created by the NPS community. Calhoun is named for Professor of Mathematics Guy K. Calhoun, NPS's first appointed -- and published -- scholarly author.

**Dudley Knox Library / Naval Postgraduate School**  
**411 Dyer Road / 1 University Circle**  
**Monterey, California USA 93943**

# NAVAL POSTGRADUATE SCHOOL Monterey, California



## THESIS

EXTENSION OF THE ANALYTICAL APPROXIMATION TO  
THE TRANSMISSION OF SOUND IN SHALLOW WATER  
USING THE IMAGE MODEL

by

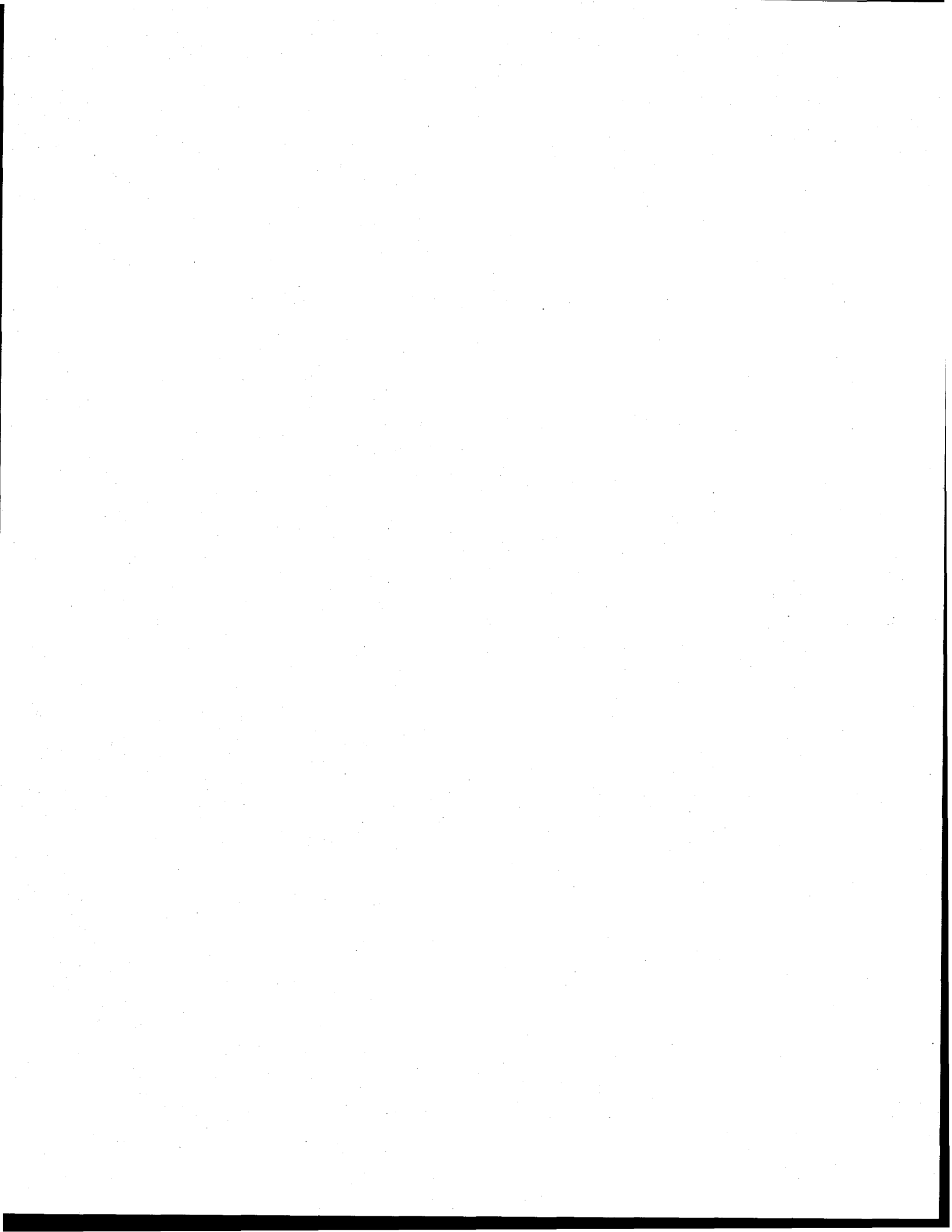
Debra M. Livingood  
September, 1992

Thesis Advisor:  
Thesis Co-advisor:

Alan B. Coppens  
James V. Sanders

Approved for public release; distribution is unlimited.

Thesis  
L71765  
c.2



REPORT DOCUMENTATION PAGE				Form Approved OMB No. 0704-0188	
1a. REPORT SECURITY CLASSIFICATION <b>UNCLASSIFIED</b>		1b. RESTRICTIVE MARKINGS			
2a. SECURITY CLASSIFICATION AUTHORITY <b>MULTIPLE SOURCES</b>		3. DISTRIBUTION / AVAILABILITY OF REPORT <b>Approved for public release; distribution is unlimited.</b>			
2b. DECLASSIFICATION / DOWNGRADING SCHEDULE		4. PERFORMING ORGANIZATION REPORT NUMBER(S)			
4. PERFORMING ORGANIZATION REPORT NUMBER(S)		5. MONITORING ORGANIZATION REPORT NUMBER(S) <b>NAVAL POSTGRADUATE SCHOOL</b>			
6a. NAME OF PERFORMING ORGANIZATION <b>NAVAL POSTGRADUATE SCHOOL</b>		6b. OFFICE SYMBOL (If applicable) <b>3A</b>	7a. NAME OF MONITORING ORGANIZATION <b>NAVAL POSTGRADUATE SCHOOL</b>		
6c. ADDRESS (City, State, and ZIP Code) <b>MONTEREY, CA 93943-5000</b>		7b. ADDRESS (City, State, and ZIP Code) <b>MONTEREY, CA 93943-5000</b>			
8a. NAME OF FUNDING / SPONSORING ORGANIZATION		8b. OFFICE SYMBOL (If applicable)	9. PROCUREMENT INSTRUMENT IDENTIFICATION NUMBER		
8c. ADDRESS (City, State, and ZIP Code)		10. SOURCE OF FUNDING NUMBERS			
		PROGRAM ELEMENT NO.	PROJECT NO.	TASK NO.	WORK UNIT ACCESSION NO.
11. TITLE (Include Security Classification) <b>EXTENSION OF THE ANALYTICAL APPROXIMATION TO THE TRANSMISSION OF SOUND IN SHALLOW WATER USING THE IMAGE MODEL</b>					
12. PERSONAL AUTHOR(S) <b>LIVINGOOD, DEBRA M.</b>					
13a. TYPE OF REPORT <b>MASTER'S THESIS</b>		13b. TIME COVERED FROM _____ TO _____	14. DATE OF REPORT (Year, Month, Day) <b>SEPTEMBER 1992</b>		15. PAGE COUNT <b>46</b>
16. SUPPLEMENTARY NOTATION <b>THE VIEWS EXPRESSED IN THIS THESIS ARE THOSE OF THE AUTHOR AND DO NOT REFLECT THE OFFICIAL POLICY OR POSITION OF THE DEPARTMENT OF DEFENSE OR THE US GOVERNMENT</b>					
17. COSATI CODES		18. SUBJECT TERMS (Continue on reverse if necessary and identify by block number)			
FIELD	GROUP	SUB-GROUP			
			<b>SHALLOW WATER MODEL, IMAGE THEORY MODEL</b>		
19. ABSTRACT (Continue on reverse if necessary and identify by block number) <b>AN ANALYTICAL APPROXIMATION TO THE IMAGE THEORY MODEL IS DEVELOPED FOR PREDICTING THE ACOUSTICAL PRESSURE FIELD IN A WEDGE-SHAPED OCEAN. THIS THESIS IS A CONTINUATION OF THE ONGOING DEVELOPMENT OF THIS MODEL. PREVIOUSLY, LIMITATIONS HAS RESTRICTED THE SOURCE AND RECEIVER TO BE PLACED IN ONLY AN UPSLOPE/DOWNSLOPE CONFIGURATION. THIS THESIS REMOVES THESE LIMITATIONS AND ALLOWS THE SOURCE AND THE RECEIVER TO BE PLACED IN CROSS-SLOPE CONFIGURATIONS.</b>					
20. DISTRIBUTION / AVAILABILITY OF ABSTRACT <input checked="" type="checkbox"/> UNCLASSIFIED/UNLIMITED <input type="checkbox"/> SAME AS RPT. <input type="checkbox"/> DTIC USERS			21. ABSTRACT SECURITY CLASSIFICATION <b>UNCLASSIFIED</b>		
22a. NAME OF RESPONSIBLE INDIVIDUAL <b>ALAN B. COPPENS</b>		22b. TELEPHONE (Include Area Code) <b>408 646-2149</b>		22c. OFFICE SYMBOL <b>PH/CZ</b>	

Approved for public release; distribution is unlimited.

Analytical Approximation to the Transmission  
of Sound in Shallow Water for Cross-Slope Propagation

by

Debra M. Livingood  
Lieutenant, United States Navy  
B.S., U.S. Naval Academy, 1986

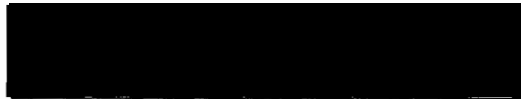
Submitted in partial fulfillment  
of the requirements for the degree of

MASTER OF SCIENCE IN APPLIED SCIENCE

from the

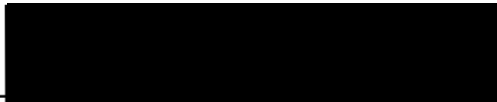
NAVAL POSTGRADUATE SCHOOL  
September 1992

Author:



Debra M. Livingood

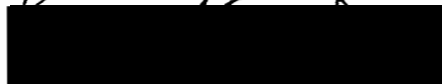
Approved by:



Alan B. Coppen, Thesis Advisor



James V. Sanders, Co-Advisor



J. N. Eagle, Chairman  
Antisubmarine Warfare Group

## ABSTRACT

An analytical approximation to the image theory model is developed for predicting the acoustical pressure field in a wedge-shaped ocean. This thesis is a continuation of the ongoing development of this model. Previously, limitations has restricted the source and receiver to be placed in only an upslope/downslope configuration. This thesis removes these limitations and allows the source and the receiver to be placed in cross-slope configurations.

1 thesis  
L717605  
C.7

## TABLE OF CONTENTS

I. INTRODUCTION . . . . .	1
II. BACKGROUND . . . . .	3
III. DEVELOPMENT . . . . .	6
A. IMAGE THEORY . . . . .	6
B. DOUBLET RADIATION . . . . .	8
C. DOUBLET ANALYSIS OF THE IMAGE THEORY . . . . .	9
1. General Description: . . . . .	9
2. Neutral Doublet ( $n=0$ ) . . . . .	12
3. Pressure Field From the Nth Pair of Acoustic Doublets . . . . .	14
a. Derivation $R'_n^+$ and $R'_n^-$ . . . . .	16
(1) The Taylor Series Expansion for $R'_n^+$ and $R'_n^-$ . . . . .	17
(2) Phase Approximation. . . . .	20
(3) Amplitude Approximation. . . . .	25
b. Derivation of $\sin\sigma'_n^+$ and $\sin\sigma'_n^-$ . . . . .	26
(1) The Taylor series expansion for $\sin\sigma'_n^+$ and $\sin\sigma'_n^-$ . . . . .	28
c. Total Pressure Including Approximations	28
4. Validation . . . . .	29

IV. CONCLUSIONS AND RECOMMENDATIONS . . . . . 32

LIST OF REFERENCES . . . . . 35

BIBLIOGRAPHY. . . . . 37

INITIAL DISTRIBUTION LIST. . . . . 39



## LIST OF FIGURES

1. Image Pattern for a Wedge-Shaped Ocean.....	7
2. 3-Dimensional View of Wedge.....	7
3. Geometrical Presentation of Doublet.....	8
4. Representation of the Groupings of Acoustical Doublets..	10
5. Geometrical Representation of Neutral Doublet.....	12
6. Geometrical Representation of $R_1$ and $\gamma$ .....	13
7. Geometrical Representation of $\sigma_0'$ and $R_0'$ .....	14
8. Geometry of Upper and Lower Doublets.....	15
9. Geometrical Representation of Upper Doublet.....	16
10. Geometrical Representation of $\sigma_{no}'$ and $R_{no}'$ .....	18
11. Geometrical Representation of $\sigma_n^+$ and $R_n^+$ .....	26

## I. INTRODUCTION

Current historical events have necessitated a change from studying the propagation of sound in deep water to studying the propagation of sound in shallow water. With the fall of the Soviet Union and the rise of Mid-Eastern countries, Antisubmarine Warfare (ASW) is more and more likely to occur in shallow water. Shallow water provides a much more complex environment for ASW prosecution, and, unfortunately, has not had as much research as in deep water.

Image theory is one method that is being developed to predict sound propagation in shallow water. This method is more accurate than ray tracing methods because it is not limited to high frequencies. A number of theses conducted at the Naval Post Graduate School were involved with applying image theory to a wedge-shaped, shallow-water ocean. The first thesis provided the groundwork for the initial development of the image theory. The most recent [Nassopoulos, 1990] derives a simplification involving a doublet approximation and incorporates all of this information into one manageable computer program [Nassopoulos, 1992].

This thesis assimilates a more complicated cross-slope approximation into the doublet analysis which allows the source and receiver to be placed anywhere in the wedge. A

computer program has also been developed to show that the approximations are correct within the set of assumptions.

## II. BACKGROUND

Research on the prediction of sound propagation in a wedge-shaped ocean has been directed in three major areas: the parabolic equation approximation, the adiabatic normal mode theory, and the image theory.

The parabolic equation can be used as a range dependent underwater acoustic propagation model. It basically replaces the Helmholtz equation with a one-way parabolic approximation which will generate the acoustic field as an initial value problem. The original version of the parabolic equation, developed in 1977 by Tappert, contained restrictions on the maximum elevation angle at the source. These limitations were reduced by Claerbout and Green and finally eliminated with the use of a higher order parabolic equation [Collins, 1987]. Because the parabolic equation is cylindrically symmetric, sloping bottoms cause a problem. One attempt to solve this problem has been attempted by sectioning off the bottom into a series of range-independent regions and then applying the normal parabolic approximation to each section [Lee et al, 1983]. Although this method increases the accuracy, it still does not alleviate the problem completely. A more recent approach to this problem has been attempted by using a rotated parabolic equation [Collins, 1990] which shows good results.

Normal mode theory is a range-independent approach. This approach has been used for open ocean predictions, but for a wedge shaped ocean, a range dependent approach is needed. For this type of approach it was shown [Pierce, 1965] that an approximation to the normal mode theory can be utilized by performing an adiabatic separation of the depth and range coordinates in the wave equation. This approach has been applied to the wedge-shaped ocean [Graves et al, 1975] but was limited to only small slopes and non-penetrable bottoms. An exact solution for the ideal wedge, where boundaries are perfectly reflected, was developed. [Buckingham, 1987] A continuing problem for adiabatic mode theory is that it can not explain the transition from the guided mode to the evanescent modes at cutoff [Jensen et al, 1980]. One hybrid approach that has been pursued to account for this is the use of the parabolic equation [Pierce, 1982] which is solved asymptotically subject to adiabatic mode initial conditions. Another method is based on tracking of local plane-wave spectra [Arnold et al, 1984] which produce intrinsic mode fields. Another method uses spectral representation based on the theory of characteristic Green's functions [Kamel et al, 1983].

Another approach in solving the wedge-shaped ocean problem is image theory. This theory predicts the pressure field from a series of projected images [Coppens et al, 1980]. A further description of this approach will be provided in the following

chapters. The basic geometry and mathematical analysis has been developed and compared to the parabolic equation model with favorable results. The upslope/downslope case has been approximated [Nassopoulos, 1992] by use of Taylor Series approximations resulting in a substantial savings in computer computational time. Although less research time has been placed into the image theory approach, it shows high potential as a viable way to predict acoustic pressure fields in a wedge shaped ocean.

### III. DEVELOPMENT

The basic goal of this research is to approximate the images by a sum of doublets. Although a full description of the theories will not be incorporated into this thesis, the following can be used as a general overview.

#### A. IMAGE THEORY

Image theory stems from the idea that if a source is radiating near a surface, then an image, out of phase with the source and an equal distance away from the surface, is produced. In an isospeed wedge-shaped ocean, numerous images are produced [MacPherson et al, 1966]. These images form a circular pattern around the point where the surface meets the bottom and interact with a series of images each possessing an image of the surface and bottom of the wedge. The images are numbered sequentially around the upper half of the circle starting with 1 for the source, 2 for the image and so on around the circle. The lower half of the circle is labeled in a similar fashion. The pattern for the sign convention along with the numbering of the images is shown in Fig. 1.

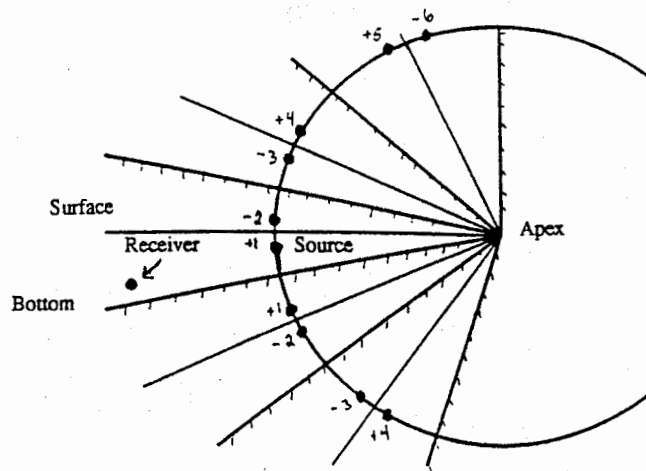
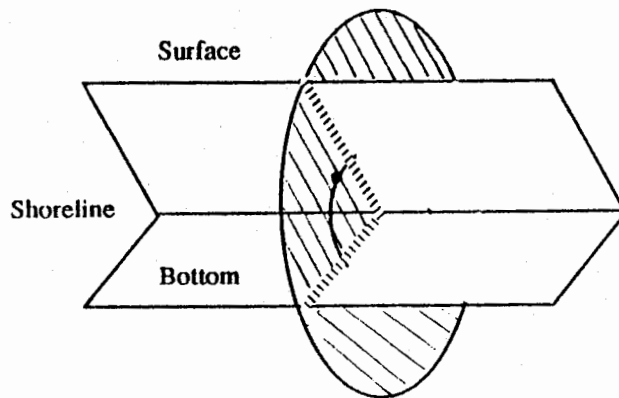


Image Pattern for a Wedge-Shaped Ocean  
Figure 1

Each image contributes to the total pressure field at a point in the wedge. For each image, the distance to the receiver and the total reflection coefficient, which is the product of all the reflection coefficients along the path from the image to the receiver, can be determined. The total pressure is the sum of the pressures from all of the images. A simplified three dimensional view at Fig. 1 shows that the shoreline acts as the perpendicular axis to the circle of images. See Fig. 2.

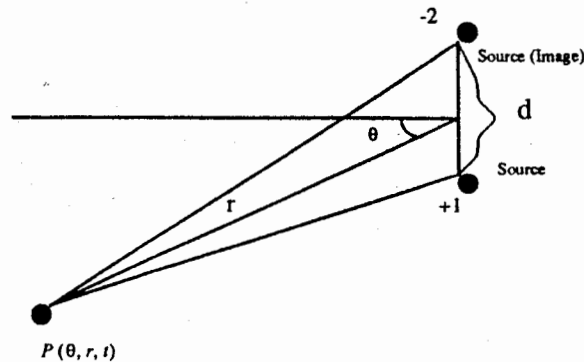


3-Dimensional View of Wedge  
Figure 2



## B. DOUBLET RADIATION

The images on each side of the pressure release surface can be grouped together in pairs to form acoustic doublets: Images 1 and 2 form a doublet, 3 and 4 form another doublet, and so on around the upper and lower half of the circle. Each doublet consists of two simple sources, vibrating at the same frequency but 180 degrees out of phase. See Fig. 3.



Geometrical Presentation of Doublet  
Figure 3

It can be shown that in the far field the pressure field resulting from this doublet using a far field approximation is

$$P(r, \theta, t) = j \frac{2A}{r} \sin\left(\frac{1}{2} k_1 d \sin\theta\right) e^{j(\omega t - kr)} \quad (1)$$

Where  $d$  is the separation of the source and image in the doublet,  $r$  is the distance from the field point to the

midpoint of the doublet, and  $\theta$  is the angle formed by  $r$  and a perpendicular bisector of the doublet. It should be noted that, if the polarities were switched, the pressure field would change sign.

To incorporate doublets into the wedge problem, Eq. 1 needs to be modified to include the reflection coefficients. Nassapolous developed the following equation for pressure

$$P(r, \theta, t) = \frac{A}{r} [(\chi - \psi) \cos\left(\frac{1}{2} k_1 d \sin\theta\right) + j(\chi + \psi) \sin\left(\frac{1}{2} k_1 d \sin\theta\right)] e^{j(\omega t - kr)} \quad (2)$$

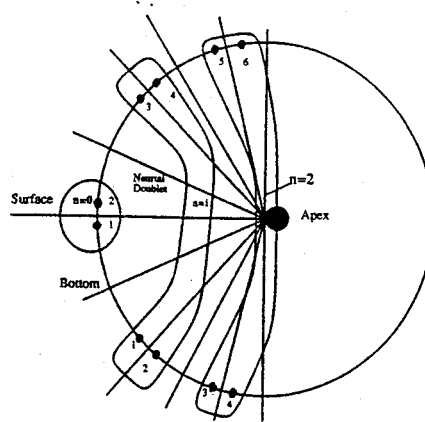
Where  $\chi$  and  $\psi$  are the cumulative reflection coefficients for the negative and positive images respectively.

### C. DOUBLET ANALYSIS OF THE IMAGE THEORY

#### 1. General Description:

The purpose of this thesis is to extend Nassapolous' doublet approximation to the image theory model to incorporate cross-slope propagation. The basic assumptions remain the same: the sound speeds and densities are constant in both the wedge and the bottom, the water-air boundary is a pressure-release surface, and the slope is constant and shallow [Nassapolous, 1992]. Nassapolous developed the case for upslope and downslope propagation. Figure 4 shows how doublets are grouped together: The third and fourth upper images are grouped together with the first and second lower images ( $n=1$ ), the fifth and sixth upper images are grouped

together with the third and fourth lower images ( $n=2$ ) and so on around the circle until all the doublets are paired.



Representation of the Groupings of Acoustical Doublets  
Figure 4

The source and image for the first surface reflected path form the neutral doublet ( $n=0$ ) and is an exception to this grouping rule. Similar to doublet radiation, where each doublet contributes to the pressure field, now, each pair of doublets is considered the basic contributor to the total pressure field. The number of paired doublets used in this total pressure calculation can be determined by

$$N = \frac{\left(\frac{360}{\beta}\right) - 2}{4} \quad (3)$$

$\beta$  is the angle between the surface and the bottom. To ensure that the pressure field is accurate, a wedge angle should be chosen such that all of the images are grouped into pairs of doublets. To insure that there is closure for the set of

images,  $360/\beta$  must be a multiple of four. In calculating the total pressure field, the pressure from the neutral doublet will first be developed, followed by the pressure field from each of the paired doublets.

All distances used are scaled according to  $R_{\text{scaled}} = R_{\text{real}}/X$ . Two bottom types are examined in this research, a fast bottom and a slow bottom. For a fast bottom, the scaling distance  $X_c$  occurs where the lowest mode attains cut off. For a slow bottom, the lowest mode does not attain cut off, but a scaling distance  $X_s$  is used for convenience in calculations. The definitions of these scaling distances are

Fast bottom:

$$\begin{aligned} K_1 X_c &= \frac{\pi}{2 \sin \theta_c \tan \beta} \\ K_2 X_c &= \frac{\pi}{2 \tan \theta_c \tan \beta} \\ \cos \theta_c &= \frac{C_1}{C_2} \end{aligned} \quad (4)$$

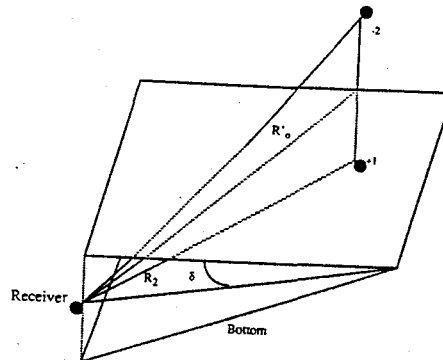
Slow bottom:

$$\begin{aligned} K_1 X_s &= \frac{\pi}{2 \tan \theta_s \tan \beta} \\ K_2 X_s &= \frac{\pi}{2 \sin \theta_s \tan \beta} \\ \cos \theta_s &= \frac{C_2}{C_1} \end{aligned} \quad (5)$$

$\beta$  is the wedge angle, the subscript 1 refers to the fluid in the water, and the subscript 2 refers to the bottom [Nassopoulos, 1992].

## 2. Neutral Doublet ( $n=0$ )

The neutral doublet, as stated above, comprises of the source and upper image. The pressure field from the neutral doublet crosses no bottom boundaries therefore, no reflection coefficients need to be considered. See Fig. 5.



Geometrical Representation of Neutral Doublet  
Figure 5

$d$  is the distance between image 1 (the source) and image 2,  $\delta$  is the angle formed between the surface and the plane containing the receiver and the shoreline, and  $R_2$  is the perpendicular distance from the shoreline to the receiver. Taking Eq. 1, that was developed for doublet radiation without reflection coefficients, and applying it to the new cross slope geometry gives

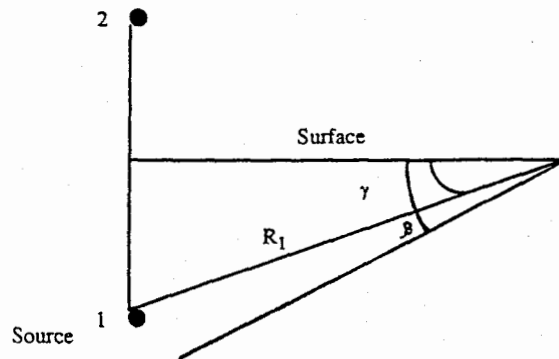
$$P_o' = j \frac{2A}{R_o'} \sin\left(\frac{1}{2} k_1 d \sin \sigma_o'\right) e^{j(\omega t - k_1 R_o')} \quad (6)$$

where  $P'_o$  is the pressure field from the neutral doublet,  $R'_o$  is the distance between the receiver and the midpoint between the neutral doublet and  $\sigma'_o$  is the angle formed between  $R'_o$  and the surface.

To reduce Eq. 6, the following substitution is made:

$$\frac{d}{2} = R_1 \sin \gamma \quad (7)$$

$\gamma$  is the angle formed between the surface plane and the plane containing the source and shoreline, and  $R_1$  is the perpendicular distance from the shoreline to the source. See Fig. 6.

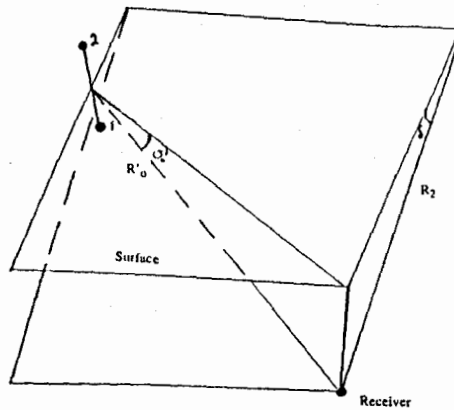


Geometrical Representation of  $R_1$  and  $\gamma$   
Figure 6

Since  $\delta$  is assumed to be a small angle,  $\sin \gamma$  can be approximated by  $\gamma$  which reduces Eq. 6 to

$$P'_o = j \frac{2A}{R'_o} \sin(k_1 R_1 \gamma \sin \sigma'_o) e^{j(\omega t - k R'_o)} \quad (8)$$

A further substitution can be made by applying the geometry in Fig. 7.



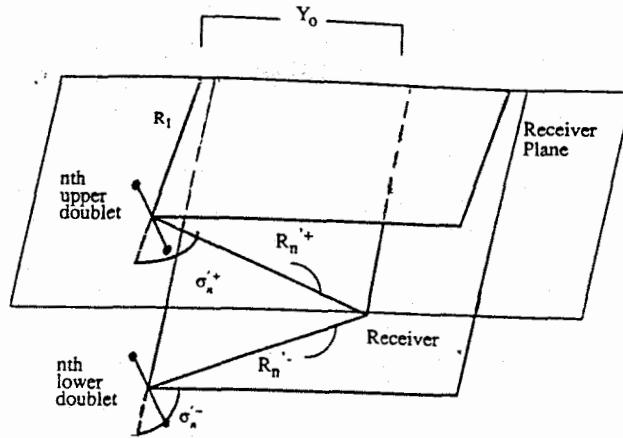
Geometrical Representation of  $\sigma'_0$  and  $R'_0$   
Figure 7

The side common to both triangles shows that  $R_2 \sin \delta = R'_0 \sin \sigma'_0$ . Since  $\delta$  is small, the small angle approximation can be utilized to form the equation  $\sin \sigma'_0 = R_2 \delta / R'_0$ . Substituting this into Eq. 8 and assigning  $\Gamma'_0 = k_1 R_1 R_2 / R'_0$  gives the final pressure for the neutral doublet

$$P'_0 = j \frac{2A}{R'_0} \sin(\Gamma'_0 \gamma \delta) e^{j(\omega t - k_1 R'_0)} \quad (9)$$

### 3. Pressure Field From the Nth Pair of Acoustic Doublets

The paired doublets can be split into two groups, one from the upper set of doublets  $P'_n^+$  and one from the lower set of doublets  $P'_n^-$ . The "" denotes the cross slope geometry, the subscript n denotes which paired doublet is being calculated and the "+" and the "-" denotes the upper and lower doublet respectively. Figure 8 illustrates the geometry of these upper and lower doublets.



Geometry of Upper and Lower Doublets  
Figure 8

The pressure from the upper doublet is

$$P_n^{'+} = (-1)^n j \frac{2A}{R_n^{'+}} \sin\left(\frac{1}{2} k_1 d \sin \sigma_n^{'+}\right) e^{j(\omega t - k R_n^{'+})} \quad (10)$$

and the pressure from the lower doublet is

$$P_n^{'-} = -(-1)^n j \frac{2A}{R_n^{'-}} \sin\left(\frac{1}{2} k_1 d \sin \sigma_n^{'-}\right) e^{j(\omega t - k R_n^{'-})} \quad (11)$$

The  $(-1)$  and the  $-(-1)$  account for the different orientations of the top and bottom doublets.

The total pressure from all of the paired doublets is

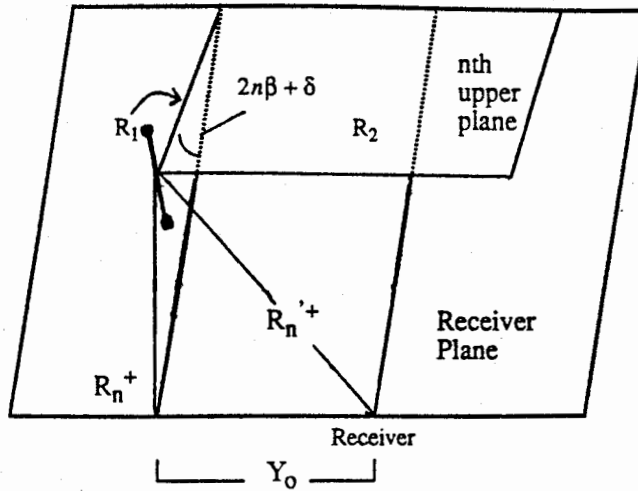
$$P_T' = P_o' + \sum_{n=1}^N P_n^{'+} + P_n^{'-} \quad (12)$$

This pressure could be calculated by a computer program, but it would take a relatively long time to compute. To shorten the computational time, and also research for an analytical approximation a Taylor series expansion is used for  $R_n^{'+}$ ,  $R_n^{'-}$ ,  $\sin \sigma_n^{'+}$ , and  $\sin \sigma_n^{'-}$ .



a. Derivation  $R_n^+$  and  $R_n^-$

The geometry for an upper doublet image is shown in Fig. 9.



Geometrical Representation of Upper Doublet

From this geometry

Figure 9

$$(R_n'^+)^2 = (R_n^+)^2 + (Y_0)^2 \quad (13)$$

and

$$(R_n^+)^2 = R_1^2 + R_2^2 - 2R_1R_2 \cos(2n\beta + \delta) \quad (14)$$

therefore by direct substitution

$$R_n'^+ = \sqrt{R_1^2 + R_2^2 + Y_0^2 - 2R_1R_2 \cos(2n\beta + \delta)} \quad (15)$$

By the same reasoning, for the lower doublet

$$R_n'^- = \sqrt{R_1^2 + R_2^2 + Y_o^2 - 2R_1R_2 \cos(2n\beta - \delta)} \quad (16)$$

Setting  $Y_o$  to zero, Eq. 15 and Eq. 16 reduce to

$$R_n'^+ = \sqrt{R_1^2 + R_2^2 - 2R_1R_2 \cos(2n\beta + \delta)} \quad (17)$$

$$R_n'^- = \sqrt{R_1^2 + R_2^2 - 2R_1R_2 \cos(2n\beta - \delta)} \quad (18)$$

which match the equations developed by Nassapolous.

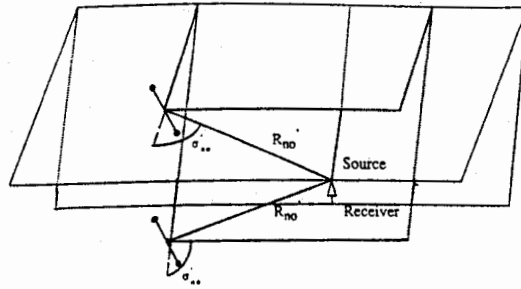
(1) *The Taylor Series Expansion for  $R_n'^+$  and  $R_n'^-$ .*

Because  $R_n'^+$  and  $R_n'^-$  appears in the phase a third order Taylor series expansion is needed. Taking this expansion around  $\delta=0$  gives

$$R_n' = R_{no}' + \delta \left. \frac{dR_n'}{d\delta} \right|_{\delta=0} + \frac{1}{2} \delta^2 \left. \frac{d^2 R_n'}{d\delta^2} \right|_{\delta=0} + \frac{1}{3!} \delta^3 \left. \frac{d^3 R_n'}{d\delta^3} \right|_{\delta=0} \quad (19)$$

This formula is the general case for both the upper and lower doublet. To get the correct formula,  $R_n'$  would be replaced with  $R_n'^+$  or  $R_n'^-$  as needed.  $R_{no}'$  is the distance to the nth doublet if the receiver were moved vertically to the surface. See Fig. 10. Since the geometry is now symmetrical

$$R_{no}'^+ = R_{no}'^- = R_{no}' = \sqrt{R_1^2 + R_2^2 + Y_o^2 - 2R_1R_2 \cos(2n\beta)} \quad (20)$$



Geometrical Representation of  $\sigma_{n0}$  and  $R_{n0}$   
Figure 10

Taking the first derivative yields

$$\frac{dR_n^{/+}}{d\delta} = \frac{R_1 R_2 \sin(2n\beta + \delta)}{R_n^{/+}} \quad (21)$$

$$\frac{dR_n^{/-}}{d\delta} = \frac{-R_1 R_2 \sin(2n\beta - \delta)}{R_n^{/-}} \quad (22)$$

$$\left. \frac{dR_n^{/+}}{d\delta} \right|_{\delta=0} = \frac{R_1 R_2 \sin(2n\beta)}{R_{n0}^{/+}} \quad (23)$$

$$\left. \frac{dR_n^{/-}}{d\delta} \right|_{\delta=0} = \frac{-R_1 R_2 \sin(2n\beta)}{R_{n0}^{/-}} \quad (24)$$

Taking the second derivative yields

$$\frac{d^2 R_n^{'+}}{d\delta^2} = \frac{[R_n^{'+} R_1 R_2 \cos(2n\beta + \delta)]}{R_n^{'+2}} - \frac{[R_1 R_2 \sin(2n\beta + \delta) R_1 R_2 \sin(2n\beta + \delta)]}{(R_n^{'+})^3} \quad (25)$$

$$\frac{d^2 R_n^{'+}}{d\delta^2} \Big|_{\delta=0} = \frac{R_1 R_2 \cos(2n\beta)}{R_{no}'} - \frac{R_1^2 R_2^2 \sin^2(2n\beta)}{R_{no}'^3} \quad (26)$$

$$\frac{d^2 R_n^{'+}}{d\delta^2} \Big|_{\delta=0} = \frac{R_1 R_2}{R_{no}'} \left[ \cos(2n\beta) - \frac{R_1 R_2 \sin^2(2n\beta)}{R_{no}'^2} \right] \quad (27)$$

Through cancellations of the minus signs, the second derivative for the lower doublet is the same, so

$$\frac{d^2 R_n^{'+}}{d\delta^2} \Big|_{\delta=0} = \frac{d^2 R_n^{'-}}{d\delta^2} \Big|_{\delta=0} \quad (28)$$

Taking the third derivative and evaluating at  $\delta=0$  yields

$$\frac{d^3 R_n^{'+}}{d\delta^3} \Big|_{\delta=0} = \frac{R_1 R_2}{R_{no}'} \left[ \frac{-3R_1 R_2 \cos(2n\beta) \sin(2n\beta)}{R_{no}'^2} - \sin(2n\beta) + \frac{3R_1^2 R_2^2 \sin^3(2n\beta)}{R_{no}'^4} \right] \quad (29)$$

$$\frac{d^3 R_n^{'-}}{d\delta^3} \Big|_{\delta=0} = -\frac{R_1 R_2}{R_{no}'} \left[ \frac{-3R_1 R_2 \cos(2n\beta) \sin(2n\beta)}{R_{no}'^2} - \sin(2n\beta) + \frac{3R_1^2 R_2^2 \sin^3(2n\beta)}{R_{no}'^4} \right] \quad (30)$$

Combining these pieces together, the third order Taylor series expansion is obtained

$$R_n'^{\pm} = R_{no}' \pm \delta \frac{R_1 R_2 \sin(2n\beta)}{R_{no}'} + \frac{1}{2} \frac{R_1 R_2}{R_{no}'} \delta^2 [\cos(2n\beta) - \frac{R_1 R_2 \sin^2(2n\beta)}{R_{no}'^2}] \pm \frac{1}{6} \frac{R_1 R_2}{R_{no}'} \delta^3 \left[ \frac{-3R_1 R_2 \cos(2n\beta) \sin(2n\beta)}{R_{no}'^2} - \sin(2n\beta) + \frac{3R_1^2 R_2^2 \sin^3(2n\beta)}{R_{no}'^4} \right] \quad (31)$$

(2) Phase Approximation.  $R_n'^+$  and  $R_n'^-$  play significant roles in the phase. Placing these terms in the phase in the third order Taylor series expansion and rearranging the terms gives

$$\exp(j\omega t) \exp \left\{ (-jk) \left[ (R_{no}') \pm \delta \frac{R_1 R_2 \sin(2n\beta)}{R_{no}'} + \frac{R_1 R_2}{2R_{no}'} \delta^2 \cos(2n\beta) - \frac{R_1 R_2 \sin^2(2n\beta)}{R_{no}'^2} \pm \frac{R_1 R_2}{6R_{no}'} \delta^3 \frac{-3R_1 R_2 \cos(2n\beta) \sin(2n\beta)}{R_{no}'^2} - \sin(2n\beta) + \frac{3R_1^2 R_2^2 \sin^3(2n\beta)}{R_{no}'^4} \right] \right\} \quad (32)$$

Since  $e^{j\omega t}$  does not contain the index  $n$ , it can be set aside for the moment and the second term will be examined for possible reductions. In order for a term to be considered negligible, a phase error of less than  $\pi/4$  is assumed. Certain assumptions also need to be made in order to represent a typical ocean environment. First, it is assumed that

$$\left| \frac{C_1 - C_2}{C_1} \right| \leq 0.1 \quad (33)$$

which is equivalent to

$$\sin\theta_c \leq 0.4 \quad (34)$$

Where  $c_1$  is the speed of sound in the water,  $c_2$  is the speed of sound in the bottom, and  $\theta_c$  is the critical angle.

Second,

$$\beta \leq 0.1 \quad (35)$$

Finally,

$$\frac{R_1}{R_{no}} \leq \frac{1}{10} \quad (36)$$

Whose implementation will be seen in the following analysis.

Grouping the terms inside the brackets from Eq. 32 in terms of powers in  $R_1$  and  $R_2$  gives

$$k \frac{R_1^3 R_2^3}{R_{no}'^5} \left[ \frac{1}{2} \sin^3(2n\beta) \delta^3 \right] \quad (37)$$

$$k \frac{R_1^2 R_2^2}{R_{no}'^3} \left[ \frac{1}{2} \sin^2(2n\beta) \delta^2 - \frac{1}{2} \cos(2n\beta) \sin(2n\beta) \delta^3 \right] \quad (38)$$

$$k \frac{R_1 R_2}{R_{no}'} \left[ \sin(2n\beta) \delta + \frac{1}{2} \cos(2n\beta) \delta^2 - \frac{1}{6} \sin(2n\beta) \delta^3 \right] \quad (39)$$

$$k R_{no}' \quad (40)$$

Each group needs to be compared to  $\pi/4$  to determine if it can be considered negligible. Beginning with expression 37 the following inequality is set up

$$k \frac{R_1^3 R_2^3}{R_{no}'^5} \left[ \frac{1}{2} \sin^3(2n\beta) \delta^3 \right] < \pi/4 \quad (41)$$

Rearranging gives

$$k \left( \frac{R_1}{R_{no}'} \right)^3 \left( \frac{R_2}{R_{no}'} \right)^2 R_2 \left[ \frac{1}{2} \sin^3(2n\beta) \delta^3 \right] < \pi/4 \quad (42)$$

Making the definitions  $S=R_1/R'_{no}$  and  $\sin\Omega=R_2/R'_{no}$  and multiplying through by  $X/X$  gives

$$kX S^3 \sin^2\Omega \frac{R_2}{X} \left[ \frac{1}{2} \sin^3(2n\beta) \delta^3 \right] < \pi/4 \quad (43)$$

where  $kX = \pi / (2 \sin\theta_c \tan\beta)$  for a fast bottom.

To ensure that the left hand side of the equation is always

$\ll \pi/4$  the maximum of all powers of sine and cosine terms will be taken to be unity, with the exception of  $\sin\theta_0$  which, as stated in the above assumptions, already has a maximum value of 0.4. Substituting these maximum values into Eq. 43 and rearranging gives

$$\frac{\pi}{.4 \tan \beta} S^3 \frac{R_2}{X} \ll \frac{\pi}{\delta^3} \quad (44)$$

Since  $\beta$  is small,  $\tan \beta = \beta$  while  $\delta$ , the receiver angle, falls between 0 and  $\beta$ . The right hand side is minimized by setting  $\beta = \delta$ . Making this substitution into Eq. 44 and allowing  $\beta$  to take on a minimum value of 0.1, reduces Eq. 44 to

$$S^3 \frac{R_2}{X} \ll 40 \quad (45)$$

Finally, substituting  $S = 1/10$  according to Eq. 36 gives

$$\frac{R_2}{X} \ll 40000 \quad (46)$$

If  $R_2/X$  for some reason became larger than 40000, the term would need to be added back into the equation to keep the phase error less than  $\pi/4$ . Note that  $\beta \geq 0.1$  is equivalent to setting a lower limit on the wedge angle of about 6 degrees. Expression 38 can be written



$$k \left( \frac{R_1}{R_{no}} \right)^2 \left( \frac{R_2}{R_{no}} \right) R_2 \left[ \frac{1}{2} \sin^2(2n\beta) \delta^2 - \frac{1}{2} \cos(2n\beta) \sin(2n\beta) \delta^3 \right] < \pi/4 \quad (47)$$

Making the same substitutions as in the previous equation yields

$$\frac{\pi}{2 \sin \theta_c \tan \beta} S^2 \frac{R_2}{X} \left[ \sin^2(2n\beta) \delta^2 - \cos(2n\beta) \sin(2n\beta) \delta^3 \right] < \pi/2 \quad (48)$$

Once again substituting in the maximizing values gives

$$S^2 \frac{R_2}{X} < 4 \quad (49)$$

Substituting  $S = 1/10$  gives

$$\frac{R_2}{X} < 400 \quad (50)$$

which allows this expression to be neglected.

Expression 39 gives

$$k \frac{R_1}{R_{no}} R_2 \left[ \sin(2n\beta) \delta + \frac{1}{2} \cos(2n\beta) \delta^2 - \frac{1}{6} \sin(2n\beta) \delta^3 \right] < \frac{\pi}{4} \quad (51)$$

Making the same substitutions as in the previous equation yields

$$\frac{\pi}{2\sin\theta_c \tan\beta} S \frac{R_2}{X} [\sin(2n\beta)\delta + \frac{1}{2}\cos(2n\beta)\delta^2 - \frac{1}{6}\sin(2n\beta)\delta^3] < \frac{\pi}{4} \quad (52)$$

Rearranging the terms and substituting in the maximum values gives

$$S \frac{R_2}{X} < \frac{.02}{\sin(2n\beta)\delta + \frac{1}{2}\cos(2n\beta)\delta^2 - \frac{1}{6}\sin(2n\beta)\delta^3} \quad (53)$$

The dominate terms in the denominator are  $\sin(2n\beta)\delta + 0.5\cos(2n\beta)\delta^2$ . Since  $1/6 \sin(2n\beta)\delta^3$  is a comparatively small number it can be neglected without increasing the phase error over  $\pi/4$ .

It follows that the expression for the upper doublet is

$$e^{-jk[R'_{no} + \frac{R_1 R_2}{R'_{no}} (\sin(2n\beta)\delta + \frac{1}{2}\cos(2n\beta)\delta^2)]} \quad (54)$$

and by the same method

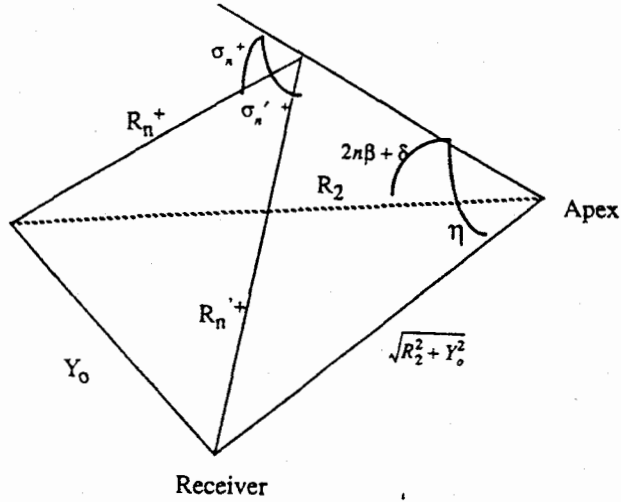
$$e^{-jk[R'_{no} - \frac{R_1 R_2}{R'_{no}} (\sin(2n\beta)\delta + \frac{1}{2}\cos(2n\beta)\delta^2)]} \quad (55)$$

for the lower doublet.

(3) *Amplitude Approximation.* It can be shown that, in the far field, the amplitude,  $R'_n$  and  $R'_n$  can be replaced by  $R'_{no}$  with a relatively small margin of error.

b. Derivation of  $\sin\sigma_n^+$  and  $\sin\sigma_n^-$

To take the Taylor series expansion of  $\sin\sigma_n^+$  and  $\sin\sigma_n^-$ , an expression for each term is needed. The geometry for this is shown in Fig. 11 for an upper doublet.



Geometrical Representation of  $\sigma_n^+$  and  $R_n^+$   
Figure 11

From the law of sines

$$\frac{R_n^+}{\sin\eta} = \frac{\sqrt{R_2^2 + Y_0^2}}{\sin\sigma_n^+} \quad (56)$$

Rearranging this gives

$$R_n^+ \sin\sigma_n^+ = \sin\eta \sqrt{R_2^2 + Y_0^2} \quad (57)$$

Substitution  $\sqrt{1 - \cos^2 \eta}$  for  $\sin \eta$  gives

$$R_n^+ \sin\sigma_n^+ = \sqrt{(R_2^2 + Y_0^2) - (R_2^2 + Y_0^2) \cos^2 \eta} \quad (58)$$

To get  $\eta$  in terms of  $\delta$  a substitution for  $\cos^2 \eta$  is needed.

To do this the following equality is setup:

$$R_n'^{+2} = R_1^2 + R_2^2 + Y_o^2 - 2R_1R_2 \cos(2n\beta + \delta) = \frac{R_1^2 + R_2^2 + Y_o^2 - 2R_1\sqrt{R_2^2 + Y_o^2} \cos \eta}{R_2^2 + Y_o^2} \quad (59)$$

Canceling similar terms and solving for  $\cos^2 \eta$  gives

$$\cos^2 \eta = \frac{R_2^2 \cos^2(2n\beta + \delta)}{R_2^2 + Y_o^2} \quad (60)$$

Substituting this into Eq. 58 and replacing  $\cos^2(2n\beta + \delta)$  with  $1 - \sin^2(2n\beta + \delta)$  gives:

$$R_n'^+ \sin \sigma_n'^+ = \sqrt{Y_o^2 + R_2^2 \sin^2(2n\beta + \delta)} \quad (61)$$

Bringing  $R_n'^+$  over to the right side gives the final expression for  $\sin \sigma_n'^+$ .

$$\sin \sigma_n'^+ = \frac{\sqrt{Y_o^2 + R_2^2 \sin^2(2n\beta + \delta)}}{R_n'^+} \quad (62)$$

And finally, by the same reasoning the expression for  $\sin \sigma_n'^-$  is

$$\sin \sigma_n'^- = \frac{\sqrt{Y_o^2 + R_2^2 \sin^2(2n\beta - \delta)}}{R_n'^-} \quad (63)$$

When the receiver is moved vertically to the surface Eq. 62 and Eq. 63 become

$$\sin \sigma_{no}' = \frac{\sqrt{Y_o^2 + R_2^2 \sin^2(2n\beta)}}{R_{no}'} \quad (64)$$

Again, by setting  $Y_o=0$  for a geometrical check

$$\sin\sigma_n^+ = \frac{R_2 \sin(2n\beta + \delta)}{R_n^+} \quad (65)$$

$$\sin\sigma_n^- = \frac{R_2 \sin(2n\beta - \delta)}{R_n^-} \quad (66)$$

which agrees with the upslope/downslope case.

(1) The Taylor series expansion for  $\sin\sigma_n^+$  and  $\sin\sigma_n^-$ . The first order Taylor series expansion taken around  $Y_0=0$  gives

$$\sin\sigma_n' = \sin\sigma_{no}' + \delta \left. \frac{d\sin\sigma_n'}{d\delta} \right|_{\delta=0} \quad (67)$$

Because these terms only appear in the amplitude, the approximation  $\sin\sigma_n' \approx \sin\sigma_{no}'$  is acceptably accurate.

### c. Total Pressure Including Approximations

Putting all of these equations together yields the pressure for the upper doublet,

$$P_n^{'+} = (-1)^{nj} \frac{2A}{R_{no}'} \left[ \sin \frac{1}{2} k_1 d \sin\sigma_{no}' \right] e^{j(\omega t)} e^{-jk_1 \left[ R_{no}' + \frac{R_1 R_2}{R_{no}'} (\sin(2n\beta)\delta + \frac{1}{2} \cos(2n\beta)\delta^2) \right]} \quad (68)$$

That for the lower doublet is the same except for a sign,

$$P_n' = -(-1)^n j \frac{2A}{R_{no}'} \left[ \sin \frac{1}{2} k_1 d \sin \sigma'_{no} \right] e^{j(\omega t)} e^{-jk_1 \left[ R_{no}' - \frac{R_1 R_2}{R_{no}'} (\sin(2n\beta) \delta + \frac{1}{2} \cos(2n\beta) \delta^2) \right]} \quad (69)$$

The pressure from the pair is

$$(-1)^n \frac{4A}{R_{no}'} \left[ \sin \frac{1}{2} k_1 d \sin \sigma'_{no} \right] e^{j(\omega t - k R_{no}')} \sin \left[ \frac{k_1 R_1 R_2}{R_{no}'} (\sin(2n\beta) \delta + \frac{1}{2} \cos(2n\beta) \delta^2) \right] \quad (70)$$

The total pressure as stated in Eq. 12 is

$$P_T' = P_o' + \sum_{n=1}^N P_n' + P_n'^- \quad (71)$$

Combining Eq. 9 and Eq. 70 gives the final solution for the total pressure,

$$P_T' = j \frac{2A}{R_o'} \sin(\Gamma_o' \gamma \delta) e^{j(\omega t - k_1 R_o')} + \sum (-1)^n \frac{4A}{R_{no}'} \left[ \sin \frac{1}{2} k_1 d \sin \sigma'_{no} \right] e^{j(\omega t - k R_{no}')} \sin \left[ \frac{k_1 R_1 R_2}{R_{no}'} (\sin(2n\beta) \delta + \frac{1}{2} \cos(2n\beta) \delta^2) \right] \quad (72)$$

#### 4. Validation

To validate the analysis of doublet cross-slope propagation, a computer program was developed. See Appendix "A". Different inputs of  $Y_o$ ,  $R_1$ , and  $R_2$  were used along with a wedge angle and source depth of 7.5 and 3.75 degrees respectively. These inputs were also put into the program URTEXT and a comparative table was constructed. See Table 1.

TABLE 1

COMPARISON OF DOUBLET ANALYSIS TO IMAGE THEORY							
$\beta = 7.5$ $\gamma = 3.75$ # of depth points = 6							
R1 = 1    R2 = 15    Y0 = 0				R1 = 1    R2 = 12    Y0 = 8			
DOUBLET		IMAGE		DOUBLET		IMAGE	
AMP	PHS	AMP	PHS	AMP	PHS	AMP	PHS
.19230	-1.189	.19020	-1.174	.20760	.97186	.14901	.99135
.37155	-1.192	.36747	-1.175	.40214	.97103	.28788	.99132
.52564	-1.195	.51973	-1.177	.57139	.96959	.40713	.99133
.64414	-1.199	.63659	-1.179	.70471	.96741	.49862	.99135
.71913	-1.203	.71006	-1.180	.79371	.96432	.55614	.99135
.74575	-1.207	.73519	-1.180	.83276	.96002	.57590	.99138
$\Delta\text{AMP} = .0066$ $\Delta\text{PHS} = .01898$				$\Delta\text{AMP} = .1729$ $\Delta\text{PHS} = .0232$			
R1 = 1    R2 = 14    Y0 = 3				R1 = 1    R2 = 8    Y0 = 9			
DOUBLET		IMAGE		DOUBLET		IMAGE	
AMP	PHS	AMP	PHS	AMP	PHS	AMP	PHS
.16437	.77749	.15456	.80884	.18308	-.2626	.12944	-.2403
.31909	.77590	.29861	.80795	.35338	-.2536	.25005	-.2402
.45507	.77353	.42229	.80677	.49899	-.2554	.35361	-.2402
.56437	.77059	.51721	.80558	.60956	-.2580	.43309	-.2403
.64061	.76720	.57687	.80473	.67701	-.2617	.48304	-.2403
.67940	.76316	.59736	.80443	.69602	-.2671	.50009	-.2403
$\Delta\text{AMP} = .0423$ $\Delta\text{PHS} = .0351$				$\Delta\text{AMP} = .1447$ $\Delta\text{PHS} = .0178$			
R1 = 1    R2 = 13    Y0 = 6				R1 = 1    R2 = 2    Y0 = 10			
DOUBLET		IMAGE		DOUBLET		IMAGE	
AMP	PHS	AMP	PHS	AMP	PHS	AMP	PHS
.19161	.77072	.14813	.74146	.00110	-.3287	.00016	-.0074
.36918	.77044	.28616	.74157	.00216	-.3376	.00030	-.0376
.51968	.76982	.40469	.74174	.00320	-.3477	.00043	-.0112
.63207	.76894	.49564	.74189	.00415	-.3607	.00052	-.0134
.69820	.76776	.55281	.74199	.00500	-.3813	.00055	-.0195
.71336	.76620	.57226	.74203	.00573	-.4041	.00055	-.0251
$\Delta\text{AMP} = .11073$ $\Delta\text{PHS} = .0272$				$\Delta\text{AMP} = .0031$ $\Delta\text{PHS} = .3421$			

It is shown that the doublet cross-slope propagation results are in good agreement with the URTEXT results. It should be noted though, that for the results to compare favorably, the wedge angle that is chosen must ensure that the number of wedges are an even multiple of four.



#### IV. CONCLUSIONS AND RECOMMENDATIONS

Image theory is an excellent method for predicting the transmission of sound in shallow water. It is an important area of research because it is directly applicable to shallow water Anti-submarine Warfare. Other methods that are being examined include the Parabolic Equation approximation, ray tracing methods, and the Adiabatic Normal Mode theory. Image theory shows the most promise for predicting the acoustical pressure fields in a wedge-shaped ocean because it can predict pressure fields for cross-slope and for all frequencies. Image theory can also deal with the transitional area at cut off, a region that is difficult for normal mode theory.

Previous theses have laid the groundwork for the image theory model. This thesis has extended the doublet approximation to cross-slope propagation. The base approximation used,  $R_1^2 \ll R_2^2 + Y_0^2$ , limits the extension to the far-field. Another limiting restriction on this thesis basically states that for a phase error of  $\pi/4$  or less, the scaled receiver distance  $R_2/X$  must be less than 400. Geometrically this says that when the receiver gets too far away the phase errors combine and the pressure equation developed in Eq. 72 is no longer valid. One further

restriction is that the wedge angle must be chosen such that the number of wedges produced is an even multiple of four. Because of this, when the dipoles are grouped into pairs of doublets, one dipole, 180 degrees from the neutral doublet, will be left ungrouped. This will only be a significant factor when the grouped dipoles cancel completely leaving only the dipole to contribute to the pressure. The effects of this dipole can also be seen in Table 1: The results vary when  $R_1$  gets small and  $Y_0$  gets large. Although this dipole can have noticeable effects on the pressure in the rigid bottom case, when reflection coefficients are incorporated, the effects become negligible.

The next step in this research would be to incorporate the reflection coefficients for the upper and lower doublet into Eq. 72. The reflection coefficients though, because of their large effect on the pressure, need to be calculated individually for each image. Nassopoulos incorporated the reflection coefficients into the upslope/downslope case, but an extension is still needed for the cross-slope case.

## APPENDIX "A"

```

10 REM WEDGE DEBBIE, DIPOLE APPROXIMATION
20 REM cross slope, wedge with rigid bottom, including third order approx
30 PI=3.1415926#
40 INPUT "angles(deg) of wedge, source: B,G =",B,G
50 INPUT "M1 = B/(delta D) =",M1
60 NPTS =INT(((INT(360/B+.0001)-2)/4)+.0001)
70 INPUT "source, receiver, apex distances: R1,R2,Y0 =",R1,R2,Y0
80 INPUT "c1/c2 =",C
90 T6=180/PI: B=B/T6: G=G/T6
100 STARCOS = SQRT(ABS(C*C-1)): T4=PI/(2*STARCOS*TAN(B))
110 LPRINT USING "THESES APPROX angles: wedge= ##.# source= ##.#":B*T6,G*T6
120 LPRINT USING "distances: source=##.## receiver=##.## shore=##.#":R1,R2,Y0
130 LPRINT USING " c1/c2= ##.# ";C
140 LPRINT USING "k1Y=pi/(2 tanB sgrabs(1-c^2))=###.###";T4
150 LPRINT USING "No. of Dipole-Pairs =##.##";NPTS
160 LPRINT " DEG AMP PHASE "
165 DIST=2*R1*SIN(G)
170 Y2=Y0+Y0: R22=R2*R2
180 C2=C*C: D2=Y0*Y0+R1*R1+R2*R2
190 R3=2*R1*R2
200 FOR M=1 TO 100: D=D+B/M1: IF (B-D)<-.0001 THEN 380
210 R0=SQRT(D2-R3*COS(D)): GAM0=R1*R2/R0
220 T=(2/R0)*SIN(T4+GAM0*G*D)
230 P1=T*SIN(T4*R0): P2=T*COS(T4*R0)
240 P3=0: P4=0
250 FOR N=1 TO NPTS
260 RN=SQRT(D2-R3*COS(2*N*B))
262 RN1=(T4*R1*R2*SIN(2*N*B))/RN
264 RN2=(T4*R1*R2*COS(2*N*B))/RN
270 SNS=(SQRT(Y2+R22*(SIN(2*N*B))^2))/RN
280 X=((-1)^N)*(2/RN)+SIN(.5*T4+DIST*SNS)
282 THDPOS= -T4*RN - D*RN1 - .5*D^2*RN2
283 THDNEG= -T4*RN + D*RN1 - .5*D^2*RN2
284 THDR = COS(THDPOS)-COS(THDNEG)
285 THDI = SIN(THDPOS)-SIN(THDNEG)
287 REAL1 = -X*THDI
289 IMAG1 = X*THDR
300 P3=REAL1 + P3
310 P4=IMAG1 + P4
320 NEXT N
330 PR=P1+P3: PIM=P2+P4
340 AMP=SQRT(PR*PR+PIM*PIM)
350 PHS=ATN(PIM/PR)
360 LPRINT USING " ##.## ##.##### ##.##### "; D*T6,AMP,PHS
370 NEXT M
380 END

```

## LIST OF REFERENCES

1. Nassopoulos, G., *Study of Sound Propagation in a Wedge-Shaped Ocean and Comparison with other Methods*, Master's Thesis, Naval Postgraduate School, Monterey, California, June 1992.
2. Collins, M.D., "Application and Time-Domain Solution of Higher-order Parabolic Equation in Underwater Acoustics," *J. Acoust. Soc. Am.*, **86**, 1097-1102, 1987.
3. Lee, D. and McDaniels, S.T., "A Finite-Difference Treatment of Interface Conditions for the Parabolic Equation: The Irregular Interface," *J. Acoust. Soc. Am.*, **73**, 1441-1447, 1983.
4. Collins, M.D., "The Rotated Parabolic Equation and Sloping Ocean Bottoms," *J. Acoust. Soc. Am.*, **87**, 1035-1037, 1990.
5. Pierce, A.D., "Extension of the Method of Normal Modes to Sound Propagation in an Almost Stratified Medium," *J. Acoust. Soc. Am.* **36**, 19-27, 1965.
6. Graves, R.D., Nagl, A., Uberall, H. and Zarur, G.L. "Range Dependent Normal Modes in Underwater Sound Propagation: Application to the Wedge-Shaped Ocean," *J. Acoust. Soc. Am.* **58**, 1171-1177, 1975.
7. Buckingham, M.J., "Theory of Three Dimensional Acoustic Propagation in a Wedge-Like Ocean with a Penetrable Bottom," *J. Acoust. Soc. Am.* **82**, 198-210, 1987.
8. Jensen, F.B. and Kuperman, W.A., "Sound Propagation in a Wedge-Shaped Ocean with a Penetrable Bottom," *J. Acoust. Soc. Am.* **67**, 1564-1566, 1980.
9. Pierce, A.D., "Guided Mode Disappearance During Upslope Propagation in Variable Depth Shallow Water Overlying A Fluid Bottom," *J. Acoust. Soc. Am.* **72**, 523-531, 1982.
10. Arnold, J.M. and Felsen, L.B., "Intrinsic Modes in a Non-Separable Ocean Waveguide," *J. Acoust. Soc. Am.* **76**, 850-860, 1984.
11. Kamel, A. and Felsen, L.B., "Spectral Theory of Sound Propagation in an Ocean Channel with Weakly Sloping Bottom," *J. Acoust. Soc. Am.* **73**, 1120-1130, 1983.

12. Coppens, A.B., Sanders, J.V., Frey, A. R. and Kinsler, L.E., *Fundamentals of Acoustics*, Third Edition, pp. 169-170, Monterey, California, January 1980.
13. Macpherson, J.D., Daintith, M.J. "Practical Model of Shallow Water Acoustic Propagation," *J. Acoust. Soc. Am.* **41**, 850-854, 1966.

## BIBLIOGRAPHY

Ansbro, A.P. and Arnold, J.M., "Numerically Efficient Evaluation of Intrinsic Modes in Wedge-Shaped Waveguides," J. Acoust. Soc. Am. **89**, 1991.

Arnold, J.M. and Felsen, L.B., "Rays and Local Modes in a Wedge-Shaped Ocean," J. Acoust. Soc. Am. **73**, 1983.

Bark, C., "The Acoustic Pressure in a Wedge-Shaped Water Overlying Fast Fluid Bottom," Master's Thesis, Naval Postgraduate School, Monterey, California, June 1992.

Bradshaw, N., "Propagation of Sound in a Fast Bottom Underlying a Wedge-Shaped Medium," Master's Thesis, Naval Postgraduate School, Monterey, California, Sept 1980.

Coppens, A.B., Humphries, M. and Sanders, J.V., "Propagation of Sound Out of a Fluid Wedge into an Underlying Fluid Substrate of Greater Sound Speed," J. Acoust. Soc. Am. **76**, 1984.

Evans, R.B., "A Coupled Mode Solution for Acoustic Propagation in a Wave-Guide With Stepwise Depth Variations of a Penetrable Bottom," J. Acoust. Soc. Am. **74**, 1983.

Green, R.R., "The Rational Approximation to the Acoustic Wave Equation with Bottom Interaction," J. Acoust. Soc. Am., **76**, 1984.

Jensen, F.B. and Tindle, C.T., "Numerical Modeling Results for Mode Propagation in a Wedge," J. Acoust. Soc. Am. **82**, 1987.

Kaswandi, C., "A computerized Investigation Using the Method of Images to Predict the Sound Field in a Fluid Wedge Overlying a Slow Half-Space," Master's Thesis, Naval Postgraduate School, Monterey, California, Dec 1987.

LeSesne, P., "Use of the Method of Images to Predict the Sound Field in a Wedge Overlying a Fast Fluid," Master's Thesis, Naval Postgraduate School, Monterey, California, Dec 1984.

Paliatsos, D., "Computer Studies of Sound Propagation in a Wedge-Shaped Ocean With Penetrable Bottom," Master's Thesis, Naval Postgraduate School, Monterey, California, March 1990.

Pierce, A.D., "Augmented Adiabatic Mode Theory for Upslope Propagation from a Point Source in a Variable-Depth Shallow Water Environments," J. Acoust. Soc. Am. **74**, 1983.

Pongsitanont, N., "Development of a Laboratory Facility for the Measurement of Sound Propagation in Shallow Water Environments," Master's Thesis, Naval Postgraduate School, Monterey, California, Dec 1989.

Rok, J.k., *Comparison of Sound Pressure in a Wedge-Shaped Ocean as Predicted By an Image Method and a PE Model*, Master's Thesis, Naval Postgraduate School, Monterey, California, Dec 1990.

Wang, L.S. and Pace, N.G., "Evaluation of the Analytic Solution for the Acoustic Field in an Ideal Wedge and the Approximate Solution in a Penetrable Wedge," *J. Acoust. Soc. Am.* **89**, 1991.

Westwood, E.K., "The Modeling of a Shallow Water Wedge Using Complex Rays and Steepest-Descent Integration," *J. Acoust. Soc. Am. Supp 1* **83**, 1988.

Yu-Ming, L., "Acoustic Pressure Distribution on the Bottom of a Wedge-Shaped Ocean," Master's Thesis, Naval Postgraduate School, Monterey, California, Dec 1987.

### INITIAL DISTRIBUTION LIST

1. Defence Technical Information Center 2  
Cameron Station  
Alexandria, VA 22304-6145
2. Library, Code 0142 2  
Naval Postgraduate School  
Monterey, CA 93943-5002
3. Department Library, Code PH 2  
Department of Physics and Chemistry  
Naval Postgraduate School  
Monterey, CA 93943-5002
4. Dr. A.B. Coppens, Code PH/CZ 2  
Department of Physics and Chemistry  
Naval Postgraduate School  
Monterey, CA 93943-5002
5. Dr J.V. Sanders, Code PH/CZ 2  
Department of Physics and Chemistry  
Naval Postgraduate School  
Monterey, CA 93943-5002
6. Lt Debra M. Livingood 2  
Surface Ship ASW Analysis Center  
Naval Station  
San Diego, CA 92136



